How will climate change spatially affect agriculture production in Ethiopia? Case studies of important cereal crops

Paul Evangelista · Nicholas Young · Jonathan Burnett

Abstract Nearly all of Ethiopia's agriculture is dependent on rainfall, particularly the amount and seasonal occurrence. Future climate change predictions agree that changes in rainfall, temperature, and seasonality will impact Ethiopia with dramatic consequences. When, where, and how these changes will transpire has not been adequately addressed. The objective of our study was to model how projected climate change scenarios will spatially and temporally impact cereal production, a dietary staple for millions of Ethiopians. We used Maxent software fit with crop data collected from household surveys and bioclimatic variables from the WorldClim database to develop spatially explicit models of crop production in Ethiopia. Our results were extrapolated to three climate change projections (i.e., Canadian Centre for Climate Modeling and Analysis, Hadley Centre Coupled Model v3, and Commonwealth Scientific and Industrial Research Organization), each having two emission scenarios. Model evaluations indicated that our results had strong predictability for all four cereal crops with area under the curve values of 0.79, 0.81, 0.79, and 0.83 for teff, maize, sorghum, and barley, respectively. As expected, bioclimatic variables related to rainfall were the greatest predictors for all four cereal crops. All models showed similar decreasing spatial trends in cereal production. In addition, there were geographic shifts in land suitability which need to be accounted for when assessing overall vulnerability to climate change. The ability to adapt to climate change will be critical for Ethiopia's agricultural system and food security. Spatially explicit models will be vital for developing early warning systems, adaptive strategies, and policy to minimize the negative impacts of climate change on food production.

IPCC   Intergovernmental Panel on Climate Change
Maxent   Maximum Entropy
EASE   Ethiopian Agriculture Sample Enumeration
GIS   Geographic Information Systems

P. Evangelista (✉) · N. Young · J. Burnett
Natural Resource Ecology Laboratory, B254 NESB, Colorado State University, Fort Collins, CO 80524-1499, USA
e-mail: paulevan@nrel.colostate.edu

Present Address:
J. Burnett
Department of Forest Engineering, Resources and Management, College of Forestry, Oregon State University, 280 Peavy Hall, Corvallis, OR 97331, USA

🍎 Springer

CCCMA   Canadian Centre for Climate Modeling and Analysis
HadCM3   Hadley Centre Coupled Model v3
CSIRO   Commonwealth Scientific and Industrial Research Organization
AUC   Area under the curve

1 Introduction

The Intergovernmental Panel on Climate Change (IPCC) defines climate change as "… a statistically significant variation in either the mean state of the climate or in its variability, persisting for an extended period; typically decades or longer (Intergovernmental Panel on Climate Change (IPCC) 2001)." Over the past 15 years, the existence, cause, and severity of climate change has been widely debated (McCright and Dunlap 2003; Oreskes 2004). However, research at the Massachusetts Institute of Technology Joint Program on the Science and Policy of Global Change indicates that, regardless of policies designed to limit anthropogenic influence, an average increase of 2 °C by 2100 is all but certain (Sokolov et al. 2009). Similar warnings by the Intergovernmental Panel on Climate Change (IPCC) (2012) predict temperatures to increase by about 1 to 3 °C by the mid-twenty-first century and by about 2 to 5 °C by the late twenty-first century. The same IPCC assessment also predicts that the frequency of heavy precipitation is likely to increase globally, even in areas where total annual rainfall is expected to decrease (Intergovernmental Panel on Climate Change (IPCC) 2012). How these changes will affect people, economies, and livelihoods remains to be seen.

It is widely held that developing countries in Africa will be particularly susceptible to climate change, in part, because of the extraordinary growth of its human population, fragility of national and regional economies, food and water insecurity, and rapid loss of natural resources (Intergovernmental Panel on Climate Change (IPCC) 2007, 2012; World Bank 2010). Furthermore, the majority of subsistence food produced in Africa comes from rain-fed agricultural systems that are dominated by small-scale subsistence farming; practices have changed little over the last few centuries. The scarcity of water and lack of irrigation systems throughout most of Africa substantially increases the dependency people have on climate for food production. Fluctuating climatic cycles (e.g., El Nino) have led to extensive drought, famine, and loss of life throughout sub-Saharan Africa (Haile 1988; Beltrando and Camberlin 1993; Nicholson and Kim 1997) and altered rainfall patterns and the subsequent loss in agricultural productivity can have direct influences on national economies (World Bank 2010), war and conflict (Raleigh and Kniveton 2012), and political stability (Raleigh 2010). Climate change is often seen as the "death knell" for many communities and countries unless farming policies can change in advance of the climate (Dinar 2007).

Of all the African countries, Ethiopia is arguably the most at risk from climate change impacts on agricultural productivity and food security. With a population exceeding 85 million people, nearly 40 % of Ethiopia's population is considered food insecure (Food and Agriculture Organization (FAO) 2009). Yet the Ethiopian economy is largely based on agriculture, which accounts for 41 % of its Gross Domestic Product, 75–80 % of exports, and 80 % of the job market (US Department of State (USDS) 2012). Ethiopia's agricultural system is highly dependent on rainfall, particularly on the amount and seasonal distribution of precipitation (Bewket 2009; Tefera 2012). Both are highly erratic and difficult to predict from year to year. Short- and long-term droughts often result in crop failures, food shortages, and devastating famines (Wood 1977). In other years, Ethiopia is known to experience

"green famines," a term used to describe seasonal shifts in rainfall patterns that result in crop failure. In some cases, rains are delayed by several weeks or may start and stop unexpectedly during critical germination periods. In either case, crops are lost while the natural vegetation is able to resume normal phenological cycles, thus providing a green landscape. When rains occur during the dry season, they facilitate the spread of crop diseases such as powdery mildew (*Erysiphe graminis*; Begassa 1985). Some studies suggest that the frequency of drought and irregular rainfall patterns in Ethiopia has increased in recent decades (Ketema 1999; Viste et al. 2013) while others predict greater consequence under future climate change (Deressa and Hassan 2009; Mideksa 2010; Intergovernmental Panel on Climate Change (IPCC) 2012). What is certain is that Ethiopia's agricultural system is already extremely vulnerable to climate, and history has repeatedly demonstrated the cascading effects of crop failure and magnitude of its consequences.

Approximately 85 % of Ethiopians live in rural areas and rely heavily on subsistence farming for survival. Family households usually cultivate areas less than 1 ha and collectively account for approximately 95 % of the country's agricultural production (Food and Agriculture Organization (FAO) 2009). Ethiopia's major food crops are cereals, which are also a principal dietary staple for most of the population. The primary cereals grown in Ethiopia are teff (*Eragrostis tef*), maize (*Zea mays*), sorghum (*Sorghum bicolor*), barley (*Hordeum vulgare*), wheat (*Triticum* spp.) and millet (*Eleusine coracana*). Cereal crops are particularly important to Ethiopia's food security. In the 2011/2012 growing season, Ethiopia produced 5,400,000 mt of maize, 3,790,000 mt of teff, 3,781,000 mt of sorghum, and 1,592,000 mt of barley (Tefera 2012). The country is one of the largest cereal producers in Africa, yet is a net importer to meet food demands. Different cereals are grown in different geographic areas and are a reflection of both climate and culture. Teff is the most preferred grain of Ethiopia and is cultivated on about 2.8 million ha (Tefera 2012). Teff is indigenous to the country and used primarily for making traditional fermented bread called *injira*. Maize is the second most common cereal grown and accounts for 36 % of all the grain production. It is a particularly important crop in rural areas where more than 80 % is consumed at the household level (Tefera 2012). In marginal lands, where average temperatures are high and rainfall is low, sorghum and millet are the primary cereals grown. Although they are the least preferred of the cereals, both are relatively drought and pest tolerant. In 2010, the Ethiopian government announced a plan to double the production of cereals by 2015; an ambitious plan considering the country's growing population, the demand for rangelands, the scarcity of water, and the extreme climates. Still, the government recently launched a campaign to convert pastoral lands and conservation areas into agriculture. However, there is no indication that cereal production is increasing but rather an emergence of foreign agribusinesses intending to grow food for export (Allaro 2012).

Surprisingly, despite the current state of Ethiopia's agricultural system and the potential impacts from climate change, there are no studies that have identified which geographic regions are most at risk. For other African countries, risk maps from projected climate change are generally coarse-scaled and lack the details needed to develop adaptive strategies that can minimize negative impacts (Thornton et al. 2009; Schlenker and Lobell 2010). Fortunately, scientists have a suite of geospatial tools and statistical models to examine ecological processes and interactions across spatial and temporal scales (Phillips et al. 2006; Elith et al. 2006). These models have demonstrated that climate is an important regional predictor for many of these ecological processes (Pearson et al. 2004; Hijmans and Graham 2006; Evangelista et al. 2008a; Kumar and Stohlgren 2009) and are being increasingly used for predicting impacts of climate change (Evangelista et al. 2011; Graham et al. 2011). In this study, our objectives were to (1) model the geographic distribution of cereal production in

Ethiopia and (2) identify how productivity may shift under multiple climate change scenarios. For our analyses, we used the relatively new Maximum Entropy (Maxent) software, a species distribution model that has become a popular and effective tool for ecologists and land managers (Evangelista et al. 2008b; York et al. 2011; Kebede et al. 2012). We tested our models on teff, maize, sorghum, and barley to represent the cereals, the diversity of livelihoods, and range of growing conditions throughout Ethiopia.

2 Methods

2.1 Study area

Our study area encompassed the country of Ethiopia located in East Africa (approximately 9° latitude and 39° longitude). With a land area of just over 1 million km^2, the country is topographically distinguished by extreme elevations ranging from −125 m to more than 4,500 m a.s.l. Mean annual temperatures range from as low as 3.9 °C in the southern highlands to as high as 31.2 °C in the Danakil desert. Annual precipitation can range from 94 to 2,228 mm largely occurring during two distinct rainy seasons, called the *belg* and *kiremet*. The *belg* occurs from March to May and is known as the short rainy season for most of Ethiopia, while the *kiremet* occurs from June to September and is known as the main rainy season. The dry season, the *bega*, normally occurs between October and January. The average duration of each season and the amount of rainfall from the *belg* and *kiremet* varies geographically (Fig. 1).

2.2 Data sources

Crop data for maize, teff, sorghum, and barley were derived from the 2002 Atlas of the Rural Ethiopian Economy (International Food Policy Research Institute (IFPRI) and Central Statistical Agency (CSA) 2006). The data were compiled following a 2001/2002 Ethiopian Agriculture Sample Enumeration (EASE) assessment. The EASE assessment was a countrywide effort to collect agricultural data by surveying 450,000 households and sampling crop types, field sizes, productivity, and household demographics across 464 *woredas* (IFPRS and International Food Policy Research Institute (IFPRI) and Central Statistical Agency (CSA) 2006; Chamberlin et al. 2007). *Woredas* are local administrative units similar to a ward or district with an average size of 2,000 km^2. Of the 583 *woredas* in Ethiopia, 119
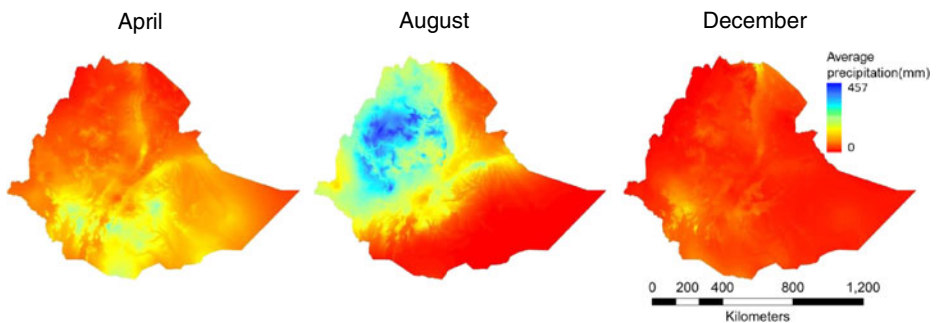
Fig. 1 Monthly rainfall (in millimeters) for 3 months representing the *belg* (short rainy season; April), the *kiremet* (main rainy season; August), and the *bega* (dry season; December)

were excluded from this study because crop data were not collected due to low human population densities and geographic remoteness. Most of the excluded *woredas* lie primarily within the Afar Region where, due to desert-like conditions, pastoralism is the dominant form of subsistence. For this analysis, the best resolution of data that was publicly available was at the *woreda* level. Crop data were acquired as a Geographic Information Systems (GIS) shapefile and processed using ArcGIS (version 10; ESRI, Redlands, CA). We selected *woredas* where quintals per hectare (qt/ha) for the specified crop were greater than or equal to the national average. These average annual yields were 7.96 qt/ha for teff, 15.10 qt/ha for maize, 12.91 qt/ha for sorghum, and 8.96 qt/ha for barley (IFPRS and CSA 2006). Within these selected *woredas*, we generated 500 random points with a minimum separation of 2 km. Quintals per hectare was selected as a proxy for crop presence because we felt actual yield was more representative of growing climate conditions and crop suitability rather than the area as a percentage of total cropped area which was also provided within the dataset.

2.3 Environmental variables

Current climate conditions were represented by 19 bioclimatic variables acquired from the WorldClim database v1.4 (Hijmans et al. 2006; www.worldclim.org). These data are available at ~1 km^2 grids which will also be the resolution of the final models and are interpolated from monthly weather station measurements collected between 1950 and 2000 (Hijmans et al. 2005). The WorldClim dataset uses altitude, temperature, and precipitation to derive monthly, quarterly, and annual climate indices to represent trends (e.g., mean diurnal temperature range), seasonality (e.g., temperature seasonality), and extremes (e.g., maximum temperature of the warmest month) that are biologically relevant (for more details, see www.worldclim.org/bioclim). Future climate scenarios were also acquired from the WorldClim database (www.worldclim.org/futdown.htm). Three different atmospheric–oceanic-coupled climate projections were used for the years 2020 and 2050. These were produced from the Canadian Centre for Climate Modeling and Analysis (CCCMA), Hadley Centre Coupled Model v3 (HadCM3), and Commonwealth Scientific and Industrial Research Organization (CSIRO). The CCCMA is a three-dimensional climate model that combines an atmospheric model and modular ocean model (Flato et al. 2000). The HadCM3 is another atmospheric-oceanic-coupled climate model is unique in that the model does not require a heat or salinity flux in its simulations to prevent drifting (Collins et al. 2001). With nine atmospheric levels and 21 vertical ocean levels, the CSIRO is another widely used coupled global climate model (Cai and Watterson 2002). Each climate projection provides two greenhouse gas emission scenarios based on the IPCC's Special Report on Emission Scenarios (Intergovernmental Panel on Climate Change (IPCC) 2001), the first representing a greater population and emissions (i.e., a2a) and the second with more conservative projections (i.e., b2a).

2.4 Analysis

We conducted our analyses using the freely available Maxent modeling software (v.3.3.3k; www.cs.princeton.edu/~schapire/maxent/), a general-purpose niche modeling algorithm for estimating probability of distributions based on the principle of maximum entropy (Phillips et al. 2004, 2006). Maxent uses point data on the landscape to identify environmental conditions based on the independent variables to predict a species' distribution excluding all conditions that are unfounded or undefined by comparing it to available environment. The model is nonlinear, nonparametric, and not sensitive to multicollinearity. Results from

the Maxent model include a spatially explicit probability surface, two model evaluations (i.e., the area under the receiving operating curve (AUC) and jackknife testing of predictor variables), and provides the permutation importance of each independent variable used to develop the model.

For each cereal crop, we developed the model based on current climate conditions and applied the defined parameters from our model results to each future climate projection (i.e., CCCMA, HadCM3, and CSIRO) and each climate scenario (i.e., 2020 A2a, 2020 B2a, 2050 A2a, and 2050 B2a). Each cereal model was developed by running 20 replicates where a random subsample of 80 % of the data was used to train the model and the remaining 20 % were withheld for testing and increasing the number of iterations per model to 5,000 to ensure model convergence. Replicates were then averaged for a final model output. The current climate predictions were reclassified to 0 (unsuitable) or 1 (suitable) using a 10 % presence logistic threshold of the training points. Future climate predictions were further reclassified to 2 (unsuitable) or 4 (suitable) and added to the current prediction to show predicted changes.

To demonstrate how each climate projection performed in our analysis, we calculated the predicted changes of unsuitable and suitable areas of each projection independently (in square kilometers). Area calculations were performed on model output grids with an equal area coordinate reference system (i.e., Africa Albers Equal Area Conic). For geographic and visual representations, we averaged the results of all three climate projections to produce change maps that differentiate areas of increasing, decreasing, and stable suitability from current to future climate scenarios.

3 Results

3.1 Teff

Under current climate conditions, suitable range for teff production is predicted highest in the north central region of Ethiopia (Fig. 2b). This largely matched the current production of teff in Ethiopia (Fig. 2a). The average test AUC for the teff production model was 0.79 with precipitation of wettest quarter (Bio16) and annual precipitation (Bio12) having the highest permutation importance of 26.6 and 19.3 %, respectively, for the final model (Table 1). Model results under averaged current climate predicted that 419,098km^2 or approximately 37 % of Ethiopia's area is suited for teff production (Appendix Table 2).

For the 2020 averaged A2a climate scenarios, the total crop area decreased to 372,577 km^2 (−11 %). Of this, our models predicted an increase of suitable crop area of 26,792 km^2 and a reduction of 73,313 km^2 from current crop area (Fig. 2c). The 2020 averaged B2a climate scenarios predicted similar results (Fig. 2d) with a total crop area decreasing to 370,379 km^2 (−12 %). Current crop area was predicted to increase by 28,475 km^2 and suitable crop area predicted to decrease by 77,193 km^2 (Appendix Table 2).

The predicted teff crop range for 2050 showed some stabilization with some additional decreases in suitable area. The averaged A2a climate scenarios for 2050 predicted the total crop range to be 349,137 km^2 (−17 %) with an increase of 41,999 km^2 and a decrease of 111,960 km^2 (Fig. 2e). The averaged B2a scenarios predicted the total crop range to decrease to 372,219 km^2, with an area suitable for teff production increasing by 35,377 km^2 and decreasing by 82,256 km^2 (Fig. 2f). All three of the future climate models and their emission scenarios produced similar results for predicted future teff production (Appendix Table 2).
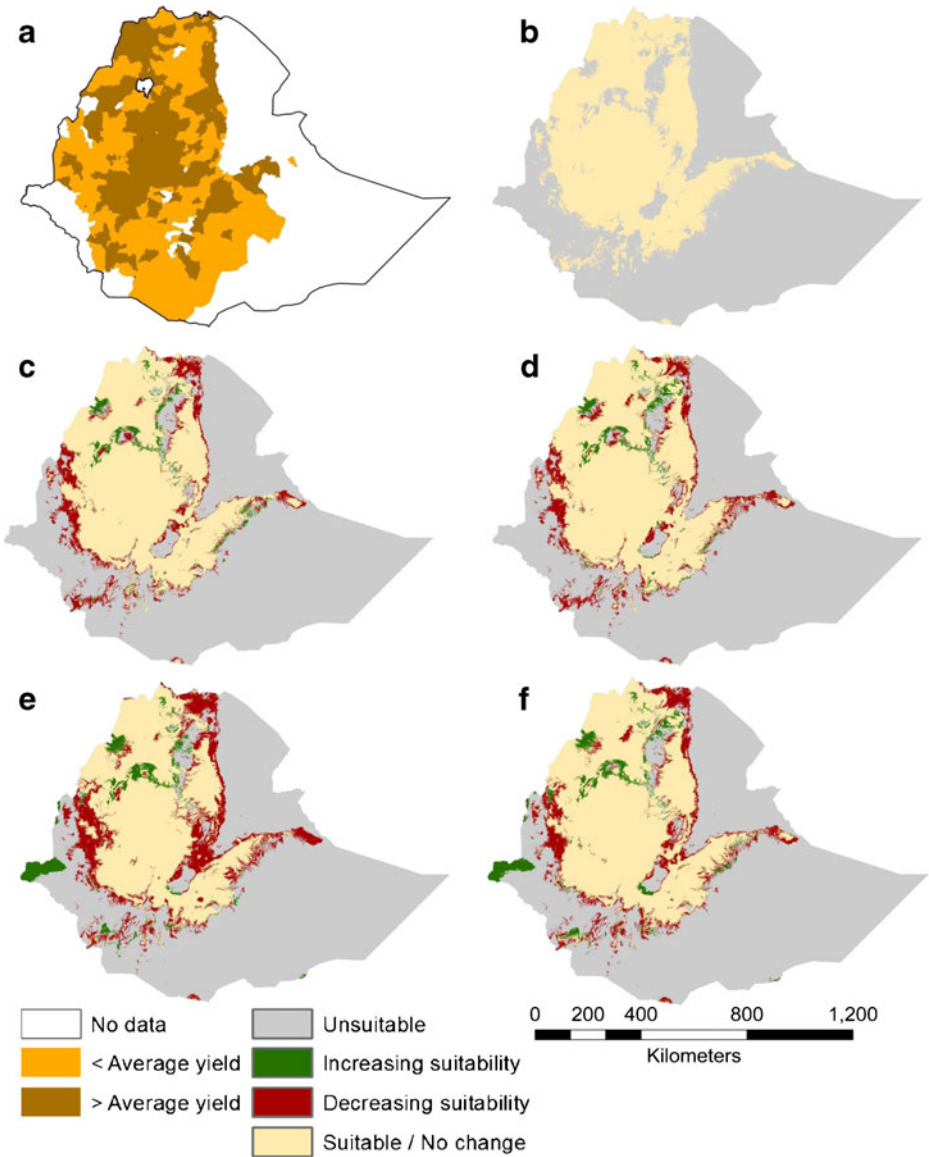
Fig. 2 Teff current production in quintal per hectare (**a**), current suitability model based on current climate (**b**), and averaged projected change in suitability for three climate models under two emission scenarios for 2 years; 2020 A2a (**c**), 2020 B2A (**d**), 2050 A2a (**e**), and 2050 B2a (**f**)

3.2 Maize

The current production of maize is highest in the northwest region of the country (Fig. 3a). Based on averaged current climate conditions, the current climate Maxent model for maize performed well with an average test AUC of 0.81. Suitable range for maize production was primarily concentrated in the western and central regions of Ethiopia. The predictor with the

Table 1 Top four predictor variables and their permutation importance in the final model for each of the four cereal crops modeled

Crop	Predictor variables	Permutation importance (%)
Teff	Precipitation of Wettest Quarter (Bio16)	26.6
	Annual precipitation (Bio12)	9.3
	Precipitation of the coldest quarter (Bio19)	8.3
	Precipitation seasonality (Bio15)	6.1
Maize	Precipitation of wettest quarter (Bio16)	32.5
	Precipitation of the driest month (Bio14)	13.5
	Precipitation seasonality (Bio15)	10.0
	Mean temperature of the wettest quarter (Bio8)	7.8
Sorghum	Annual precipitation (Bio12)	36.0
	Precipitation of the driest month (Bio14)	9.3
	Temperature Seasonality (Bio4)	8.7
	Precipitation of Wettest Month (Bio13)	6.0
Barley	Annual precipitation (Bio12)	26.3
	Precipitation of Wettest Quarter (Bio16)	9.8
	Min Temperature of Coldest Month (Bio6)	9.2
	Temperature Seasonality (Bio4)	7.9

highest permutation importance for the modeled distribution was precipitation of wettest quarter (Bio16) having a contribution of 32.5 %. The second highest contributing predictor was precipitation of the driest month (Bio14) with a contribution of 13.5 % (Table 1). Current models predicted that 358,624 km^2 or approximately 32 % of the landscape is suitable for maize production (Fig. 3b; Appendix Table 3).

For the 2020 averaged A2a climate scenarios, the total crop area decreased to 306,691 km^2 (−14 %). Of this, the model predicted an increase of suitable crop area by 24,805 km^2 and a reduction by 76,739 km^2 from current crop area (Fig. 3c). The 2020 averaged B2a climate scenarios predicted slightly lower suitable area with a total crop area decreasing to 283,211 km^2 (−21 %). Current crop area was predicted to increase by 24,518 km^2, and suitable crop areas are predicted to decrease by 99,931 km^2 under this scenario (Fig. 3d; Appendix Table 3).

The predicted trend for A2a is continued to decrease suitable area for maize by 2050 while the trend for B2a is predicted to stabilize or slightly increase. The A2a- and B2a-averaged scenarios for 2050 predicted that the suitable range for maize production will be 268,806 and 295,061 km^2, respectively. For the A2a climate scenarios, the crop area is predicted to increase by 22,634 km^2 from the current range and decrease by 112,453 km^2 (Fig. 3e). Similarly, the averaged B2a climate scenarios predicted crop area to increase by 29,888 km^2 and decrease by 93,451 km^2 (Fig. 3f). All three of the future climate models (i.e., HADCM3, CCCMA, and CSIRO) showed decreases in suitable area for maize with CCCMA having the greatest decreases and CSIRO having the least (Appendix Table 3).
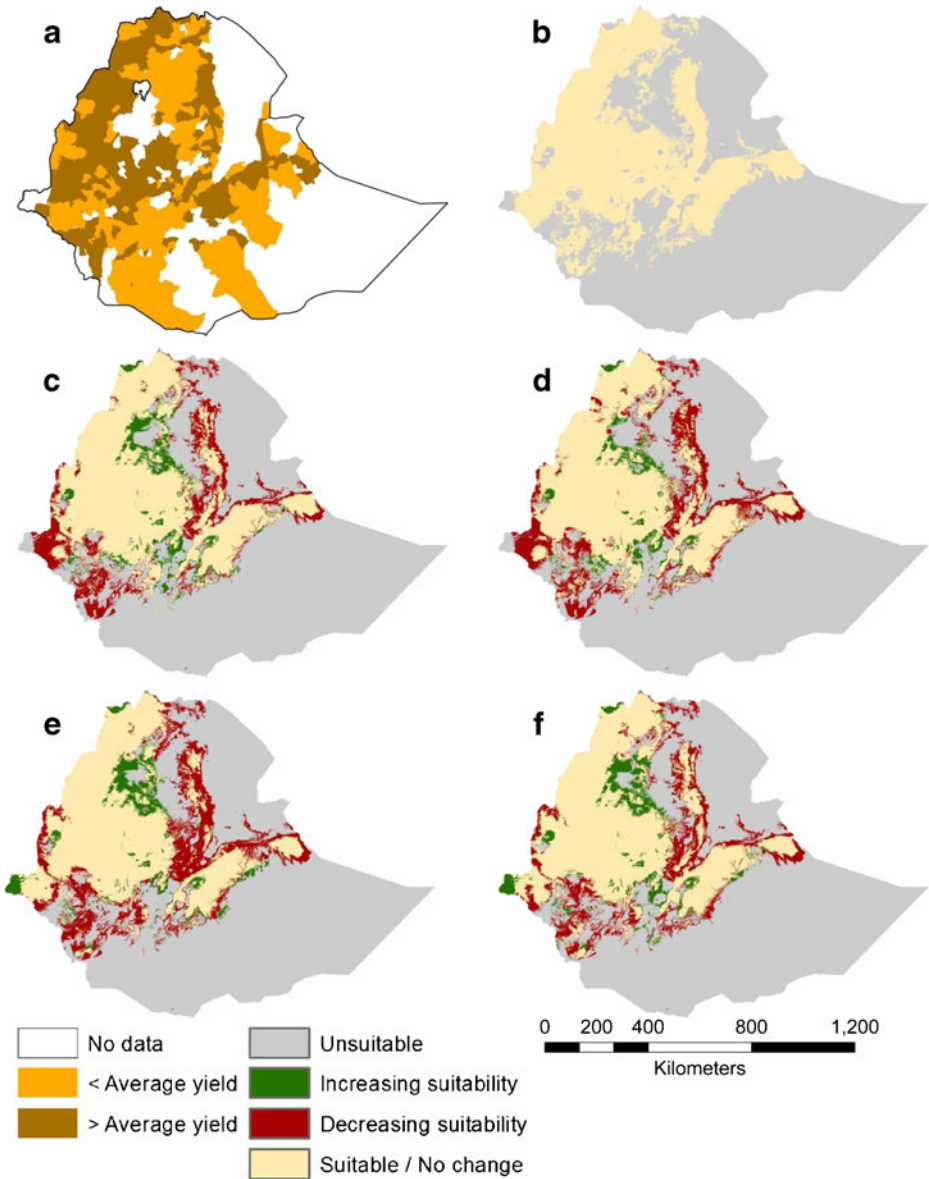
3.3 Sorghum

The highest production for sorghum is concentrated centrally and along the northwestern border of Ethiopia (Fig. 4a). Under current climate conditions, predicted suitable range for
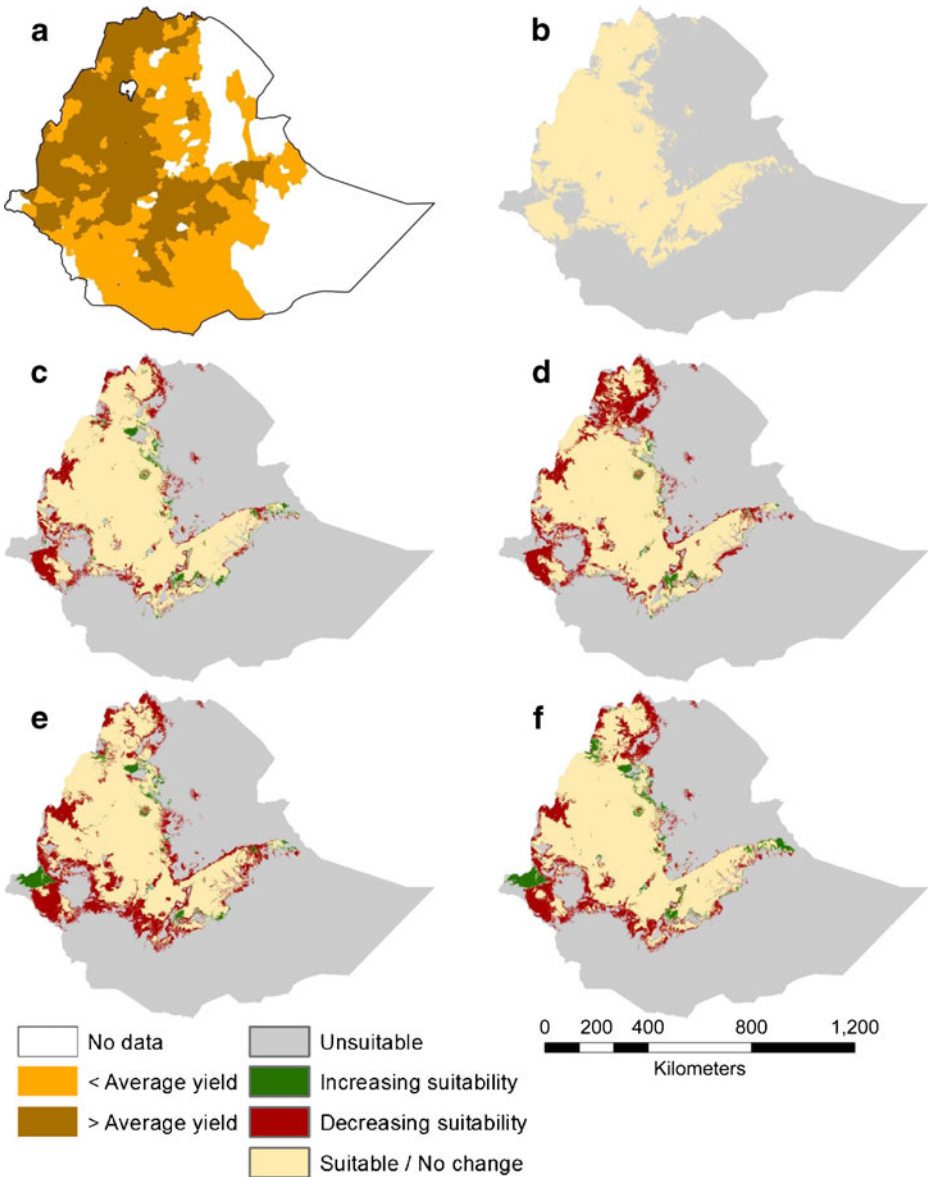
Fig. 3 Maize current production in quintal per hectare (**a**), current suitability model based on current climate (**b**), and averaged projected change in suitability for three climate models under two emission scenarios for 2 years; 2020 A2a (**c**), 2020 B2A (**d**), 2050 A2a (**e**), and 2050 B2a (**f**)

sorghum production is highest in western to northern Ethiopia and in central Ethiopia (Fig. 4b), aligning with the current production yields. The average test AUC for the sorghum model was 0.79 with annual precipitation (Bio12) and precipitation of the driest month (Bio14) having the highest contributions of 36.0 and 9.3 % to the final results, respectively (Table 1). Model results for the current climate predicted 415,773 km^2 or approximately 37 % of Ethiopia's area is suited for sorghum production (Appendix Table 4).

Fig. 4 Sorghum current production in quintal per hectare (**a**), current suitability model based on current climate (**b**), and averaged projected change in suitability for three climate models under two emission scenarios for two years; 2020 A2a (**c**), 2020 B2A (**d**), 2050 A2a (**e**), and 2050 B2a (**f**)

For the 2020-averaged A2a climate scenarios, the total crop area decreased to 385,858 km^2 (−7 %). Of this, suitable crop area is predicted to increase from current predictions by 50,858 km^2 and decrease by 80,500 km2 (Fig. 4c; Appendix Table 4). The 2020-averaged B2a climate scenarios predicted similar results with a total crop area decreasing to 366,964 km^2 (−12 %). Of the total crop area for 2020 B2a, suitability for sorghum production is predicted to increase by 46,212 km^2 and decrease by 95,021 km^2 (Fig. 4d).

The predicted crop range for 2050 A2a was 385,183 km^2 (−7 %), almost exactly the same as the 2020 A2a scenario. The predicted increase of crop range was 62,909 km^2, while the decrease in area was 93,499 km^2 (Fig. 4e). The averaged 2050 B2a climate scenarios predicted the total crop range to increase from 2020 predictions to 401,506 km^2 but was still slightly less than current predictions (−3 %). The predicted suitable area for sorghum production under the 2050 B2a scenario increased by 60,940 km^2 and decreased by 75,208 km^2 (Fig. 4f). All three of the future climate models and their emission scenarios had similar results in predicted future sorghum production (Appendix Table 4).
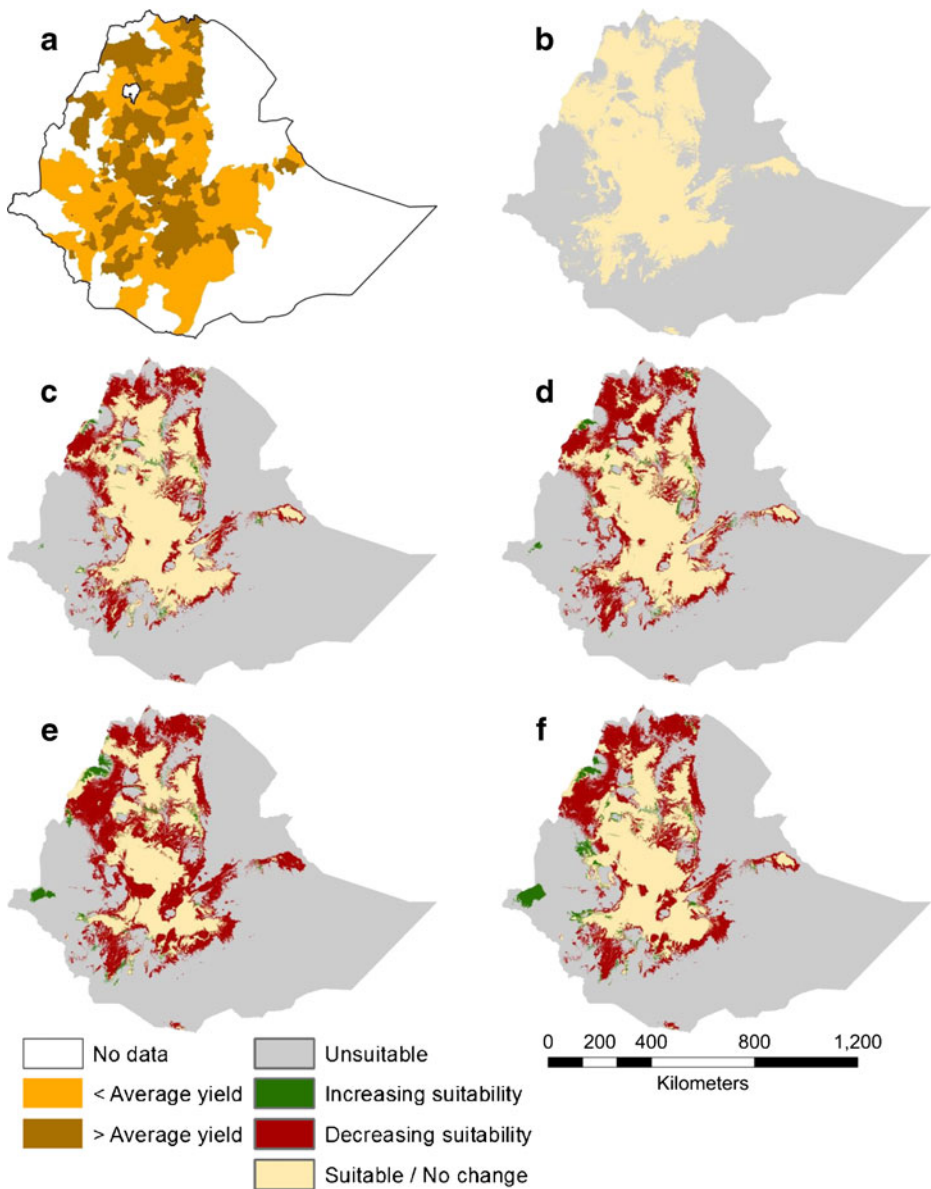
3.4 Barley

Current barley production is highest in the north central region of Ethiopia (Fig. 5a). Predicted suitable range for barley production based on average current climate conditions was primarily concentrated to the northwest and central regions of Ethiopia, agreeing with those regions of higher yield in current production (Fig. 5b). The average test AUC for the barley crop production model was 0.83 with annual precipitation (Bio12) having the highest predictive importance at 26.3 % (Table 1). The second strongest predictor was the precipitation of the wettest quarter (Bio16) with a permutation importance of 9.8 % (Table 1). Current models predicted that 350,766 km^2 or approximately 31 % of the landscape is suitable climate for barley production (Fig. 5b; Appendix Table 5).

Under the 2020 A2a climate scenario, the averaged three climate projections total crop area for barley dramatically decreased to 221,763 km^2 (−31 %). Of this, our models predicted an increase of suitable crop area of only 19,668 km^2 and a decrease of 129,003 km^2 from current suitable crop area (Fig. 5c). The 2020 B2a climate scenarios also predicted significant range decreases with a total suitable barley crop area of 224,470 km^2 (−36 %; Fig. 5d). Current crop area was predicted to increase by 20,886 km^2 and decrease by 147,182 km^2 from current climate predictions (Appendix Table 5).

Decreasing crop areas were predicted to continue by 2050. The A2a- and B2a-averaged scenarios for 2050 predicted that the total suitable range for barley production will be 190,040 (−46 %) and 220,507 km^2 (−37 %), respectively (Fig. 5e). For the A2a climate scenarios, the crop area is predicted to increase by 23,887 km^2 and decrease by 184,613 km^2 from the current climate range prediction. The averaged B2a climate scenarios predicted crop area to increase by 30,216 km^2 and decrease by 160,475 km^2 (Fig. 5f). The CCCMA climate model for all emission scenarios predicted significantly higher decreases in future suitable area for barley production compared with HadCM3 and CSIRO (Appendix Table 5).

4 Discussion

Our model evaluations for the current climate averages indicate strong model performances and predictability for all four cereal crops. We were also encouraged that the future HadCM3, CCCMA and CSIRO climate predictions for each crop showed similar trends among the different climate assessments and emission scenarios. We also noticed that the top climatic predictors for each crop (Table 1) corresponded with the growing conditions described in the literature and by rural farmers in Ethiopia (Evangelista, personal communication). These, with the strong AUC evaluations, lead us to believe that our models provide reasonable predictions on the geographic changes in cereal production throughout Ethiopia under projected climate change. However, we advise that our results be interpreted with prudence due to a number of untested and untestable assumptions we had to make

Fig 5 Barley current production in quintal per hectare (**a**), current suitability model based on current climate (**b**) and averaged projected change in suitability for three climate models under two emission scenarios for 2 years; 2020 A2a (**c**), 2020 B2A (**d**), 2050 A2a (**e**), and 2050 B2a (**f**)

related to environmental conditions in space and time. All models have associated assumptions and extrapolating models in time or space is subject to violating assumptions of species distribution models (Wiens et al. 2009). We consider our results as probable future scenarios that relate crop production and climate from a select number of intensive studies and observed trends. The models relied on predicted future climate scenarios, which add an immeasurable degree of uncertainty to our results and are difficult to validate (Beaumont et

al. 2007). We must also keep in mind that Ethiopia commonly experiences erratic climate patterns, which are expected to increase in time (Deressa and Hassan 2009; Mideksa 2010). Fluctuations in climate, seasonally or annually, are not reflected in our analyses though we are quite certain that it would intensify the impacts associated with our predictions.

Ethiopia is generally known for its fertile soils, though variations in composition and structure occur geographically. Soils are a significant influence on cereal productivity, and we believe they may have strengthened our model predictions if included in our analyses. Unfortunately, we were unable to find suitable soils data for our study. Soils, however, can be modified and improved as needed through different means, such as fertilizing, fallowing, crop rotation, and terracing. So despite the absence of soils in our models, we do not believe it diminishes the value and trends of our results. There are numerous natural and anthropogenic variables that are known to facilitate or regulate crop production, which could either compound the negative effects of climate change or provide opportunities for adaptation and increased resilience. These range from insect outbreaks, farming practices, new technologies, market prices, traditional preference, conflict, and others that simply cannot be projected or confidently integrated in our models (Heikkinen et al. 2006; Schlenker and Lobell 2010).

Further research is recommended to refine predictions and better assess the potential impacts that climate change may have on agricultural production. Of particular importance is the need for better spatial datasets. As previously noted, there remain large data gaps that restrict our ability to predict productivity at finer scales. These include information collected at community and landscape scales and span a wide range of disciplines. There is also a need for alternative means of testing model performance and predictions beyond traditional statistical evaluations. The use of species distribution models in real-time studies allows researchers to validate results in the field; however, this is not an option when trying to predict environmental responses to future climate change. One alternative approach would be to test models using historical climate records to predict current conditions. Unfortunately, the absence of historical data for developing countries such as Ethiopia is particularly problematic but may be tested in countries where such datasets exist and is available.

Despite varying degrees of uncertainty, our results provide detailed quantitative predictions that are spatially and temporally explicit. Because climate change will affect different communities and crops disproportionately, the types and intensity of adaptive strategies required will need to be assessed on a regional basis. Broad national-scale climate forecasts (e.g., Schlenker and Lobell 2010) for a country that is as culturally and ecologically diverse as Ethiopia simply have little or no value to end-users at local or regional scales. Models, such as the ones we present here, are critical for determining the vulnerability of specific targets, whether it is a specific crop, a resource, or a community. Ultimately, we hope this study and our results demonstrates the need and importance of a spatially explicit early warning system that will inform research, decision-making processes, adaptive management, and development to minimize the negative impacts of climate change on food production.

5 Conclusions

Even under conservative emission scenarios, future climate changes are expected to significantly reduce Ethiopia's cereal production. All of our models, projected to the HadCM3,

CCCMA, and CSIRO climate model projections, showed similar decreasing trends for the four cereal crops. Barley was predicted to have the greatest reductions, with net losses in land area ranging from 28 to 62 % (Appendix Table 5). Sorghum had the least change, ranging from a net loss of 21 % to a net gain of 14 % (Appendix Table 4). In addition to net losses and gains of land area, there were dramatic geographic shifts in land suitability that need to be accounted for when assessing overall vulnerability. All models had reasonably high AUC values indicating strong performances. As expected, predictability with all of our models largely centered on rainfall patterns and seasonality. Based on multiple future climate projections, our results support the many studies warning of future risks to Ethiopia's food security.

Appendices

Table 2 Predicted areas (in square kilometers) for teff production using (1) historic 50-year climate averages and (2) three future climate projections (i.e., HadCM3, CCCMA, and CSIRO) averaged and independently

	Total range	Stable	Increase	Decrease
Current climate prediction	419,098			
Averaged (HadCM3, CCCMA, and CSIRO)				
2020 a2a	372,577 (−11)	345,785 (83)	26,792 (6)	73,313 (−17)
2020 b2a	370,379 (−12)	341,904 (82)	28,475 (7)	77,193 (−18)
2050 a2a	349,137 (−17)	307,138 (73)	41,999 (10)	111,960 (−27)
2050 b2a	372,219 (−11)	336,842 (80)	35,377 (8)	82,256 (−20)
HadCM3				
2020 a2a	382,095 (−9)	349,409 (83)	32,686 (8)	69,689 (−17)
2020 b2a	365,593 (−13)	339,508 (81)	26,085 (6)	79,590 (−19)
2050 a2a	344,384 (−18)	283,554 (68)	60,830 (15)	135,544 (−32)
2050 b2a	378,975 (−10)	344,419 (82)	34,556 (8)	74,679 (−18)
CCCMA				
2020 a2a	370,545 (−12)	342,445 (82)	28,099 (7)	76,653 (−18)
2020 b2a	357,871 (−15)	328,781 (78)	29,090 (7)	90,317 (−22)
2050 a2a	361,083 (−14)	318,577 (76)	42,506 (10)	100,520 (−24)
2050 b2a	345,213 (−18)	317,044 (76)	28,169 (7)	102,053 (−24)
CSIRO				
2020 a2a	365,090 (−13)	345,500 (82)	19,590 (5)	73,598 (−18)
2020 b2a	387,674 (−7)	357,424 (85)	30,249 (7)	61,673 (−15)
2050 a2a	341,944 (−18)	319,282 (76)	22,662 (5)	99,816 (−24)
2050 b2a	392,469 (−6)	349,062 (83)	43,407 (10)	70,036 (−17)

The percent change from current climate predictions are provided in parenthesis

Table 3 Predicted areas (in square kilometers) for maize production using (1) historic 50-year climate averages and (2) three future climate projections (i.e., HadCM3, CCCMA, and CSIRO) averaged and independently

	Total range	Stable	Increase	Decrease
Current climate prediction	358,624			
Averaged (HadCM3, CCCMA, and CSIRO)				
2020 a2a	306,691 (−14)	281,886 (79)	24,805 (7)	76,739 (−21)
2020 b2a	283,211 (−21)	258,694 (72)	24,518 (7)	99,931 (−28)
2050 a2a	268,806 (−25)	246,171(69)	22,634 (6)	112,453 (−31)
2050 b2a	295,061 (−18)	265,174 (74)	29,888 (8)	93,451 (−26)
HadCM3				
2020 a2a	317,128 (−12)	291,972 (81)	25,156 (7)	66,653 (−19)
2020 b2a	282,007 (−21)	262,656 (73)	19,351 (5)	95,968 (−27)
2050 a2a	256,577 (−28)	231,782 (65)	24,795 (7)	126,843 (−35)
2050 b2a	301,523 (−16)	272,732 (76)	28,790 (8)	85,892 (−24)
CCCMA				
2020 a2a	274,006 (−24)	253,382 (71)	20,624 (6)	105,242 (−29)
2020 b2a	234,901 (−34)	223,886 (62)	11,015 (3)	134,738 (−38)
2050 a2a	241,645 (−33)	224,529 (63)	17,116 (5)	134,095 (−37)
2050 b2a	238,503 (−33)	228,996 (64)	9,507 (3)	129,628 (−36)
CSIRO				
2020 a2a	328,940 (−8)	300,304 (84)	28,636 (8)	58,320 (−16)
2020 b2a	332,726 (−7)	289,539 (81)	43,186 (12)	69,085 (−19)
2050 a2a	308,195 (−14)	282,203 (79)	25,992 (7)	76,421 (−21)
2050 b2a	345,158 (−4)	293,793 (82)	51,365 (14)	64,832 (−18)

The percent change from current climate predictions are provided in parenthesis

Table 4 Predicted areas (in square kilometers) for sorghum production using (1) historic 50-year climate averages and (2) three future climate projections (i.e., HadCM3, CCCMA, and CSIRO) averaged and independently

	Total range	Stable	Increase	Decrease
Current climate prediction	415,773			
Averaged (HadCM3, CCCMA, and CSIRO)				
2020 a2a	385,858 (−7)	335,273 (81)	50,585 (12)	80,500 (−19)
2020 b2a	366,964 (12)	320,752 (77)	46,212(11)	95,021 (−23)
2050 a2a	385,183 (−7)	322,274 (78)	62,909 (15)	93,499 (−22)
2050 b2a	401,506 (−3)	340,565 (82)	60,940 (15)	75,208 (−18)
HadCM3				
2020 a2a	393,663 (−5)	334,105 (80)	59,558 (14)	81,668 (−20)
2020 b2a	355,530 (14)	307,147 (74)	48,383 (12)	108,626 (−26)
2050 a2a	386,258 (−7)	312,987 (75)	73,272 (18)	102,786 (−25)
2050 b2a	410,422 (−1)	342,590 (82)	67,832 (16)	73,183 (−18)

Table 4 (continued)

	Total range	Stable	Increase	Decrease
CCCMA				
2020 a2a	380,558 (−8)	331,054 (80)	49,504 (12)	84,719 (−20)
2020 b2a	329,903 (−21)	298,080 (72)	31,823 (8)	117,693 (−28)
2050 a2a	363,363 (−13)	303,510 (73)	59,853 (14)	112,263 (−27)
2050 b2a	375,762 (−10)	321,910 (77)	53,852 (13)	93,863 (−23)
CSIRO				
2020 a2a	383,352 (−8)	340,659 (82)	42,693 (10)	75,114 (−18)
2020 b2a	415,460 (0)	357,031 (86)	58,429 (14)	58,742 (−14)
2050 a2a	405,929 (−2)	350,326 (84)	55,603 (13)	65,447 (−16)
2050 b2a	418,333 (1)	357,196 (86)	61,137 (15)	58,577 (−14)

The percent change from current climate predictions are provided in parenthesis

Table 5 Predicted areas (in square kilometers) for barley production using (1) historic 50-year climate averages and (2) three future climate projections (i.e., HadCM3, CCCMA, and CSIRO) averaged and independently

	Total range	Stable	Increase	Decrease
Current climate prediction	350,766			
Averaged (HadCM3, CCCMA, CSIRO)				
2020 a2a	241,431 (−31)	221,763 (63)	19,668 (6)	129,003 (−37)
2020 b2a	224,470 (−36)	203,584 (58)	20,886 (6)	147,182 (−42)
2050 a2a	190,040 (−46)	166,153 (47)	23,887 (7)	184,613 (−53)
2050 b2a	220,507 (−37)	190,292 (54)	30,216 (9)	160,475 (−46)
HadCM3				
2020 a2a	253,349 (−28)	230,038 (66)	23,311 (7)	120,728 (−34)
2020 b2a	146,522 (−58)	126,029 (36)	20,493 (6)	224,738 (−64)
2050 a2a	204,679 (−42)	175,445 (50)	29,235 (8)	175,322 (−50)
2050 b2a	220,507 (−37)	190,292 (54)	30,216 (9)	160,475 (−46)
CCCMA				
2020 a2a	171,531 (−51)	161,657 (46)	9,875 (3)	189,110 (−54)
2020 b2a	133,433 (−62)	125,739 (36)	7,694 (2)	225,027 (−64)
2050 a2a	180,965 (−48)	155,844 (44)	25,121 (7)	194,922 (−56)
2050 b2a	180,418 (−49)	164,909 (47)	15,509 (4)	185,857 (−53)
CSIRO				
2020 a2a	294,326 (−16)	266,905 (76)	27,421 (8)	83,861 (−24)
2020 b2a	286,629 (−18)	254,976 (73)	31,653 (9)	95,791 (−27)
2050 a2a	242,632 (−31)	216,586 (62)	26,046 (7)	134,181 (−38)
2050 b2a	276,425 (−21)	230,521 (66)	45,904 (13)	120,245 (−34)

The percent change from current climate predictions are provided in parenthesis

References

Allaro HB (2012) The effect of export-led growth strategy on the Ethiopian economy. Amer J Econ 2(3):50–56

Beaumont LJ, Pitman AJ, Poulsen M, Hughes L (2007) Where will species go? Incorporating new advances in climate modeling into projections of species distributions. Glob Change Biol 13:1368–1385

Begassa M (1985) Geographic distribution and genotypic diversity of resistance to powdery mildew of barley in Ethiopia. Hereditas 102(1):113–121

Beltrando G, Camberlin P (1993) Interannual variability of rainfall in the eastern Horn of Africa and indicators of atmospheric circulations. Int J Climatol 13:533–546

Bewket W (2009) Rainfall variability and crop production in Ethiopia: case study in the Amhara region. In: Ege S, Aspen H, Teferra B, Bekele S (eds) Proceedings of the 16th International Conference of Ethiopian Studies. Trondheim, Norway

Cai W, Watterson IG (2002) Modes of interannual variability of the Southern Hemisphere circulation simulated by the CSIRO climate model. J Clim 15(10):1159–1174

Chamberlin J, Tadesse M, Benson T, Zakaria S (2007) Atlas of the Ethiopian rural economy: expanding the range of available information for development planning. Inf Dev 23:181–192

Collins M, Tett SFB, Cooper C (2001) The internal climate variability of HadCM3, a version of the Hadley Centre coupled model without flux adjustments. Clim Dynam 17(1):61–81

Deressa TT, Hassan RM (2009) Economic impact of climate change on crop production in Ethiopia: evidence from cross-section measures. J Afr Econ 18(4):529–554

Dinar A (2007) The Final Blow for Agriculture in Africa? World Bank Development Research group. Available from http://econ.worldbank.org/WBSITE/EXTERNAL/EXTDEC/EXTRESEARCH/0,,contentMDK:21425514~pagePK:64165401~piPK:64165026~theSitePK:469382~isCURL:Y,00.html. Accessed 19 April 2010

Elith J, Graham C, Anderson R, Dudik M, Ferrier S, Guisan A, Hijmans R, Huettmann F, Leathwick J, Lehmann A, Li J, Lohmann L, Loiselle B, Manion G, Moritz C, Nakamura M, Nakazawa Y, Overton J, Peterson AT, Phillips S, Richardson K, Scachetti-Pereia R, Schapire R, Soberon J, Williams S, Wisz M, Zimmermann N (2006) Novel methods improve prediction of species distributions from occurrence data. Ecography 29(2):129–151

Evangelista P, Norman J III, Behanu L, Kumar S, Alley N (2008a) Predicting habitat suitability for the endemic mountain nyala (*Tragelaphus buxtoni*) in Ethiopia. Wildl Res 35:409–416

Evangelista P, Kumar S, Stohlgren TJ, Jarnevich CS, Crall AW, Norman JB III, Barnett D (2008b) Modeling invasion for a habitat generalist and a specialist plant species. Divers Distrib 14:808–817

Evangelista P, Kumar S, Stohlgren T, Young N (2011) Assessing forest vulnerability and the potential distribution of three pine beetles under current and future climate scenarios in the Interior West of the U.S. For Ecol Manag 262(3):307–316

Flato GM, Boer GJ, Lee WG, McFarlane NA, Ramsden D, Reader MC, Weaver AJ (2000) The Canadian Centre for Climate Modelling and Analysis global coupled model and its climate. Clim Dynam 16(6):451–467

Food and Agriculture Organization (FAO) (2009) Country profile: food security indicators country: Ethiopia. Available from http://www.fao.org/fileadmin/templates/ess/documents/food_ security_statistics/country_ profiles/eng/Ethiopia_E.pdf. Accessed 14 April 2010

Graham J, Jarnevich C, Young N, Newman G, Stohlgren T (2011) How will climate change affect the potential distribution of Eurasian tree sparrows *Passer montanus* in North America? Acta Zool Sin 57(5):648–654

Haile T (1988) Causes and characters of drought in Ethiopia. Ethiop J Agr Sci 10(1–2):85–97

Heikkinen RK, Miska L, Araujo MB, Virkkala R, Thuiller W, Sykes MT (2006) Methods and uncertainties in bioclimatic envelope modeling under climate change. Prog Phys Geog 30:751–777

Hijmans RJ, Graham CH (2006) The ability of climate envelope models to predict the effect of climate change on species distributions. Glob Chang Biol 12:2272–2281

Hijmans RJ, Cameron SE, Parra JL, Jones PG, Jarvis A (2005) Very high resolution interpolated climate surfaces for global land areas. Inter J Climatol 25:1965–1978

Hijmans RJ, Cameron SE, Parra JL (2006) WorldClim Global Climate Layers Version 1.4. Available from WorldClim Database: http://www.worldclim.org. Accessed 11 November 2011

Intergovernmental Panel on Climate Change (IPCC) (2001) Climate Change 2001: The Scientific Basis, Contribution of Working Group I to the Third Assessment Report of the Intergovernmental Panel on Climate Change. Houghton JT, Ding Y, Griggs DJ, Noguer M, van der Linden PJ, Dai X, Maskell K, Johnson CA (ed) Cambridge University Press, Cambridge, 881 pp.

Intergovernmental Panel on Climate Change (IPCC) (2007) Climate change 2007: Impacts, Adaptation and Vulnerability. Contribution of Working Group II to the Fourth Assessment Report of the Intergovernmental Panel on Climate Change. Parry ML, Canziani OF, Palutikof JP, van der Linden PJ, and Hanson CE (ed) Cambridge University Press. Cambridge, UK, p 976

Intergovernmental Panel on Climate Change (IPCC) (2012) Managing the Risks of Extreme Events and Disasters to Advance Climate Change Adaptation. A Special Report of Working Groups I and II of the Intergovernmental Panel on Climate Change. Field CB, Barros V, Stocker TF, Qin D, Dokken DJ, Ebi KL, Mastrandrea, MD, Mach KJ, Plattner GK, Allen SK, Tignor M, Midgley PM (ed) Cambridge University Press, Cambridge, UK and New York, NY, USA, pp 582

International Food Policy Research Institute (IFPRI) and Central Statistical Agency (CSA) (2006) Atlas of the Ethiopian rural economy. Library of Congress, Washington, DC

Kebede F, Bekele A, Moehlman P, Evangelista P (2012) Endangered Grevy's zebra in alledeghi wildlife reserve, ethiopia: species distribution modeling for the determination of optimum habitat for management. Endanger Species Res 17:237–244

Ketema T (1999) Test of homogeneity, frequency analysis of rainfall data and estimate of drought probabilities in Dire Dawa, eastern Ethiopia. Ethiop J Nat Resour 1:125–136

Kumar S, Stohlgren TJ (2009) Maxent modeling for predicting suitable habitat for threatened and endangered tree Canacomyrica monticola in New Caledonia. J Ecol Nat Environ 1:94–98

McCright AM, Dunlap RE (2003) Defeating Kyoto: the conservative movement's impact on U.S. climate change policy. Soc Probl 50(3):348–373

Mideksa TK (2010) Economic and distributional impacts of climate change: the case of Ethiopia. Global Environ Chang 20:278–286

Nicholson S, Kim J (1997) The relationship of ENSO to African rainfall. Int J Climatol 17:117–135

Oreskes N (2004) Beyond the ivory tower; the scientific consensus on climate change. Science 306(5702):1686

Pearson RG, Dawson TP, Liu C (2004) Modelling species distributions in Britain: a 20 hierarchical integration of climate and land-cover data. Ecography 27:285–298

Phillips SJ, Dudik M, Schapire RE, (2004) A maximum entropy approach to species distribution modeling. In: Proceedings of the 21st 27 International Conference on Machine Learning. ACM Press, New York, NY, USA, pp 655–662

Phillips SJ, Anderson RP, Schapire RE (2006) Maximum entropy modeling of species geographic distributions. Ecol Model 190:231–259

Raleigh C (2010) Political marginalization, climate change, and conflict in African Sahel States. Rev Int Stud 12:69–86

Raleigh C, Kniveton D (2012) Come rain or shine: an analysis of conflict and climate variability in East Africa. J Peace Res 49(1):51–64

Schlenker W, Lobell D (2010) Robust negative impacts of climate change on African agriculture. Environ Res Lett 5:1–8

Sokolov AP, Stone PH, Forest CE, Prinn RG, Sarofim MC, Webster M, Paltsev S, Schlosser CA, Kicklighter D, Dutkiewicz S, Rielly J, Wang C, Felzer B, Melillo J, Jacoby HD (2009) Probabilistic forecast for 21st century climate based on uncertainties in emissions (without policy) and climate parameters. J Climate 22:5175–5204

Tefera A (2012) Ethiopia: Grain and Feed Annual Report. Global Agricultural Information Network. USDA Foreign Agriculture Service, Report Number ET 1201. Available from http://gain.fas.usda.gov/USDS, 2012. Accessed 8 October 2012

Thornton P, Jones P, Alagarswamy G, Andresen J (2009) Spatial variation of crop yield response to climate change in East Africa. Global Environ Chang 19:54–68

US Department of State (USDS) (2012) Background note: Ethiopia. Bureau of African Affairs. Available from http://www.state.gov/r/pa/ei/bgn/2859.htm. Accessed 8 October 2011

Viste E, Korecha D, Sorteberg A (2013). Recent drought and precipitation tendencies in Ethiopia. Theor Appl Climatol (in press)

Wiens JA, Stralberg D, Jongsomjit D, Howell CA, Snyder MA (2009) Niches, models, and climate change: assessing the assumptions and uncertainties. [Proceedings Paper]. Proc Nat Acad Sci USA 106:19729–19736

Wood A (1977) A preliminary chronology of Ethiopian droughts. In: Dalby D, Church RJH, Bezzaz F (eds) Drought in Africa, vol 2. International African Institute, London, pp 68–73

World Bank (2010) Economics of Adaptation to Climate Change: Ethiopia. The World Bank Group, Washington DC, p 124

York P, Evangelista P, Kumar S, Graham J, Flather C, Stohlgren T (2011) A Habitat Overlap Analysis derived from Maxent for Tamarisk and the Southwestern Willow Flycatcher. Front Earth Sci 5(2):120–129